JOURNAL OF Applied Polymer SCIENCE

Synthesis of Nanosized Ethylene–Propylene Rubber Latex via Polyisoprene Hydrogenation

Anong Kongsinlark,[1] Garry L. Rempel,[2] Pattarapan Prasassarakich[3,4]

[1]Program in Petrochemistry and Polymer Science, Faculty of Science, Chulalongkorn University, Bangkok 10330, Thailand
[2]Department of Chemical Engineering, University of Waterloo, Ontario, Canada N2L3G1
[3]Department of Chemical Technology, Faculty of Science, Chulalongkorn University, Bangkok 10330, Thailand
[4]Center for Excellence on Petrochemical and Materials Technology, Chulalongkorn University, Bangkok 10330, Thailand

Correspondence to: G. L. Rempel (E-mail: grempel@uwaterloo.ca)
and P. Prasassarakich (E-mail: ppattara@chula.ac.th)

ABSTRACT: Nanosized ethylene–propylene rubber (EPM) latex with a particle size of 47 nm was synthesized via an alternative route consisting of isoprene (IP) polymerization followed by hydrogenation. First, the IP monomer was polymerized by differential microemulsion polymerization to obtain polyisoprene (PIP) rubber latex with a particle size of 42 nm. The structure of synthetic PIP was hydrogenated at the carbon–carbon double bonds to produce an ethylene–propylene copolymer by diimide reduction in the presence of hydrazine and hydrogen peroxide using boric acid as promotor. The degree of hydrogenation was determined by proton nuclear magnetic resonance (^{1}H-NMR) spectroscopy and the structure of the ethylene–propylene copolymer was identified by ^{13}C-NMR spectroscopy. In nanosized PIP hydrogenation, the hydrogenation level was found to be increased by boric acid addition. An EPM yield of 94% was achieved using a hydrogen peroxide : hydrazine ratio of 1.5 : 1. The EPM produced from PIP has high thermal stability with the maximum decomposition temperature of 510°C and a glass transition temperature of -42.4°C close to commercial ethylene–propylene diene rubber. Dynamic mechanical analysis indicated that EPM had a maximum storage modulus due to the saturated carbons domains of the ethylene segments in the polymer chains. © 2012 Wiley Periodicals, Inc. J. Appl. Polym. Sci. 000: 000–000, 2012

KEYWORDS: ethylene-propylene rubber; diimide hydrogenation; polyisoprene; nanoparticle

Received 30 March 2012; accepted 1 April 2012; published online 00 Month 2012
DOI: 10.1002/app.37883

INTRODUCTION

The synthesis of thermoplastic polymers with elastomeric properties has received much attention in scientific research and industrial production. Ethylene–propylene rubber (EPM) and ethylene–propylene diene (EPDM) rubber, a class of thermoplastic elastomers, are one of the most versatile, fastest growing, and interesting synthetic rubbers. EPM is well known to have higher oxidative stability and better environmental stability and thermal properties than those of diene-based elastomers, such as, polybutadiene rubber or polyisoprene (PIP) rubber, due to the absence of unsaturated bonds in their polymer backbones.[1,2] The importance of ethylene–propylene copolymers is increasing strongly based on its superiority in resistance to oxygen, ozone and weathering resistance, chemical inertness, and lightness of color.[3,4] The ethylene–propylene copolymers could be processed with a number of additives and could be the most widely used elastomer for specialty applications, such as, in the automotive industry, rubber mechanical goods and construction materials, and impact modifiers for coatings and engineering plastics.[5–8] Industrially, there are three major commercial processes for manufacturing EPMs: solution, suspension, and gas phase. For the solution polymerization process, ethylene and propylene are polymerized using catalysts in a hydrocarbon solvent, such as, a hexane or heptanes.[9] For the suspension process, EPDM as linear synthetic elastomeric interpolymer was prepared employing liquid propylene and cyclohexane and using a transition metal compound activated with an organometallic reducing agent.[10]

For the gas-phase polymerization, ethylene and propylene gas together with catalyst are fed into a fluidized-bed reactor.[11] It is well known that EPM and EPDM were produced by polymerization with Ziegler–Natta catalysts. Ver Strate et al.[12] reported the preparation of ethylene–propylene copolymers using

Additional Supporting Information may be found in the online version of this article.

vanadium halide catalysts with premixing of the aluminum alkyl and vanadium components prior to contacting with the monomers, and narrow molecular weight distribution copolymer was obtained. The catalysts of $TiCl_4/MgCl_2/PCl_3$ and $TiCl_4/MgCl_2/(n\text{-}Bu)_3PO_4$ were used for producing ethylene–propylene copolymer resulting in high propylene incorporation in the copolymer and very low crystallinity.[13] Recently, metallocene catalysts were developed for the copolymerization of ethylene and propylene. The metallocene catalysts [metallocene activated with methylalumoxane (MAO) and metallocene complexes of MAO/rac-$Me_2Si[2Me\text{-}Ind]_2ZrCl_2$ on silica support] were found to be highly selective and yielded copolymer with controlled stereoregularity, and with good control for the ethylene to propylene ratio.[14,15]

From earlier work, the synthesis of EPM required gas monomers equipment, organic solvent with solvent recovery, and a metal catalyst. Hence, an alternative way is proposed for the synthesis of EPM nanoparticle by hydrogenation of nanosized PIP in the absence of a solvent and a metal catalyst providing a "new green process." The method of diimide hydrogenation of carbon–carbon double bonds in a latex system was employed and diimide generated from the reaction between hydrazine and hydrogen peroxide could be used to provide hydrogen for hydrogenation.[16] Diimide reduction has been applied for the hydrogenation of carbon–carbon double bonds within acrylonitrile–butadiene rubber (NBR) with a hydrogenation degree of 81%,[17] carboxylated styrene butadiene rubber (XSBR) with a hydrogenation degree of 80%,[18] and natural rubber latex (NRL) with a hydrogenation degree of 67%.[19,20] However, a low degree of hydrogenation of NR was obtained due to the larger size of the rubber particles (0.2–2 μm).

Commercial NRL (1–2 μm), skim natural rubber (0.2–1 μm), and XSBR (0.1 μm) have relatively large particle size. In recent years, polymer nanoparticles have become an attractive field of research due to the novel properties of such nanomaterials. The extraordinarily large surface area on the nanoparticle and the high stability of nanomaterials could present diverse opportunities and improvement of mechanical, electrical, and thermal properties.[21–23] Based on previous work on nanosized rubber, nanosized PIP with an average particle size of 27 nm was synthesized by differential microemulsion polymerization using 2,2-azoisobutyronitrile as initiator.[24] Differential microemulsion polymerization has been applied in which the monomer is continuously and slowly added as very small droplets to the polymerization system under mild agitation. The differential microemulsion polymerization is controllable in providing nanoparticles of less than 20 nm at an extremely low surfactant amount, which is difficult to be realized by conventional emulsion polymerization.[25] Nanosized styrene/butadiene block copolymer has been synthesized by a reversible addition–fragmentation chain transfer seeded emulsion polymerization to obtain a particle size in the range of 50–80 nm.[26]

In the present work, ethylene-*co*-propylene rubber latex was synthesized via diimide hydrogenation of synthetic PIP nanoparticle. First, the PIP nanoparticles were synthesized by differential microemulsion polymerization, and the nanosized PIP so obtained was then hydrogenated by diimide reduction in a water system using hydrazine reacted with hydrogen peroxide and boric acid as promoter. Differential microemulsion polymerization is advantageous methods for the production of PIP nanoparticles with an extremely low-surfactant concentration, and diimide hydrogenation is normally performed using an environmental friendly process due to the absence of organic solvents and metal catalyst. The influences of process variables on PIP hydrogenation and the dynamic mechanical properties of EPM were investigated.

EXPERIMENTAL

Materials

Isoprene (IP) and sodium bicarbonate (NaHCO3) purchased from Aldrich (St. Louis, MO, USA), sodium persulfate (SPS) purchased from Sigma (St. Louis, MO, USA) and sodium dodecyl sulfonate (SDS) purchased from Fisher Scientific (Fair Lawn, NJ, USA) were used as received for nanosized PIP synthesis. Hydrazine hydrate and boric acid purchased from Aldrich (St. Louis, MO, USA) and hydrogen peroxide (30% aqueous solution) purchased from VWR Scientific (Toronto, ON, Canada) were used as received for the diimide hydrogenation. Methyl ethyl ketone (MEK) was obtained from Fisher Scientific (Fair Lawn, NJ, USA) for rubber precipitation and d-chloroform (99.9%) was purchased from Aldrich Chemical (St. Louis, MO, USA) for NMR analysis. Deionized water was used in all experiments.

Synthesis of PIP Nanoparticles

PIP nanoparticles were synthesized by differential microemulsion polymerization. The differential microemulsion polymerization of IP was performed in a 250-mL Parr reactor. A total of 0.2 g of SPS initiator, 0.6 g SDS, and 0.7 g sodium bicarbonate were dissolved in deionized water (70 mL) and charged into the reactor. The solution was stirred at 300 rpm under a nitrogen atmosphere. Then, the mixture was heated to the desired reaction temperature of 75°C and then condensed IP monomer (20 g) was fed via small dropwise addition continuously using a peristaltic pump at a feeding rate of 0.8 mL/min. After the addition of the monomer was completed, the reaction system was held at a constant temperature (75°C) and stirring rate (300 rpm) for 18 h.

Diimide Hydrogenation for EPM Synthesis

PIP latex was used as the starting reactant for diimide hydrogenation. The hydrogenation of nanosized PIP latex in the presence of a hydrazine/hydrogen peroxide system was conducted in a 250-mL glass reactor equipped with a temperature controlled oil bath, reflux condenser, a nitrogen gas inlet, and a feeding tube. The deionized water (10 mol/L) was added into the PIP latex and charged into the glass reactor. Then, hydrazine hydrate (5 mol/L) and dissolved boric acid (0.15 mol/L) were dropped into the latex. Then, nitrogen gas was charged for degassing the reaction system before heating up to the reaction temperature. Subsequently, the mixture was heated up to the desired temperature and hydrogen peroxide (7.5 mol/L) was added dropwise using a peristaltic pump at a feeding rate of 0.4 mL/min at a constant temperature. When the addition of hydrogen peroxide was completed, the reaction was left to proceed for 4 h under a constant stirring rate. The synthetic EPM latex thus produced was then precipitated using MEK to form the coagulated rubber.

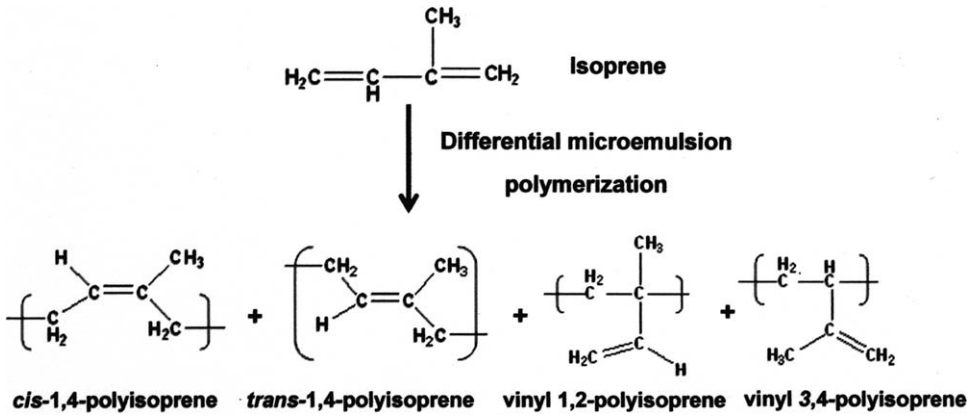

Figure 1. Structure configurations of synthetic PIP nanoparticles.

Characterization

The actual final degree of hydrogenation or PIP conversion was examined by proton nuclear magnetic resonance (^{1}H-NMR) spectroscopy. The structure identification was interpreted from ^{13}C-NMR spectroscopy. The hydrogenated PIP (HPIP) was dissolved in $CDCl_3$ at room temperature and the spectra were recorded on an Advance Bruker 300 MHz spectrometer. For the determination of particle size, the z-average diameter and size distribution of HPIP nanoparticles were measured using a dynamic light scattering technique (Malvern Instrument).

For thermal analysis, the initial decomposition temperature (T_{id}) and the temperature at the maximum of mass loss rate were determined using a Perkin–Elmer Pyris Diamond thermogravimetric/differential thermal analysis instrument (TG/DTA). A sample weight of 10 mg was placed on a platinum pan and the temperature was raised from room temperature to 800°C under a nitrogen atmosphere at a flow rate of 50 mL/min and the heating rate for all experiments was 15°C/min.

Dynamic mechanical thermal analysis of PIP and HPIP was performed using a dynamic mechanical thermal analyzer (METTLER) in a shear mode. The loss tangent (tan δ) curve is determined to obtain the glass transition temperature (T_g). All samples were analyzed with a strain of 70-μm peak to peak displacement. The temperature was run at an oscillation frequency of 10 Hz with a heating rate of 5°C/min. The hydrogenated rubber samples were cut as strips with dimensions of 12 × 12 × 2 mm^3.

The solid content of EPM was measured gravimetrically and calculated according to eq. (1)

$$\%\text{DRC} = (M_1/M_2) \times 100, \quad (1)$$

where M_1 mass of dry coagulated rubber (g), M_2 mass of the latex sample (g).

RESULTS AND DISCUSSION

Characterization of PIP Nanoparticles

The PIP nanoparticles synthesized via differential microemulsion polymerization had an average particle size of 42 nm with a narrow size distribution of polydispersity index equal to 0.02. The configurations of PIP were in four structures of the IP unit, 1,4-*cis*, 1,4-*trans*, 1,2-vinyl, and 3,4-polyisoprene as shown in Figure 1. The qualitative and quantitative analysis of the functional groups of PIP were identified by ^{1}H-NMR spectroscopy as shown in Figure 2(a). A signal was observed at 5.15 ppm corresponding to olefinic protons of *cis*- and *trans*-1,4-polyisoprene. The methine proton of 1,2-vinyl polyisoprene was identified at 5.7 ppm, whereas the signal in the range of 4.60–4.80 ppm was the characteristic peak of the methylene proton of 3,4-polyisoprene. The ratio of structures was calculated from the integrated peak areas of these signals; therefore, synthetic PIP was composed of 1,4-polyisoprene, 1,2-polyisoprene, and 3,4-polyisoprene with an average ratio of 91 : 3 : 6. For the aliphatic protons, a high intensity peak at 1.58 and 1.67 ppm was attributed to methyl protons of *cis*-1,4- and *trans*-1,4-polyisoprene, respectively. The appearance of 1,4 addition peaks was calculated resulting in an approximate ratio of *cis*-1,4 to *trans*-1,4 of 80 : 20. The characteristic peak of the methylene groups for 1,4 addition appeared in the range of 1.95–2.15 ppm, moreover the low intensity peaks at 0.95 and 1.3 ppm could be assigned to methyl protons of 1,2-polyisoprene and 3,4-polyisoprene, respectively.

Characterization of EPM Nanoparticles

The conversion of PIP to ethylene–propylene copolymer was determined in terms of the hydrogenation degree, the increase in hydrogenation degree resulted in an increase in the EPM yield. The hydrogenation degree of HPIP was determined using ^{1}H-NMR spectroscopy as shown in Figure 2(b,c). The actual percentage of hydrogenation was calculated from the peak area of the olefinic protons (C=C) and the integrated peak area over the range of 0.8–2.0 ppm. From Figure 2(b), when diimide hydrogenation proceeded to 78% hydrogenation, the signals at 5.7 and 4.7 ppm corresponding to olefinic protons of 1,2-vinyl polyisoprene and 3,4-polyisoprene were greatly decreased. The integrated peak area of *cis*-, *trans*-olefinic protons of 5.15 ppm gradually decreased with the increasing degree of hydrogenation. New peaks appearing at 0.8 ppm attributed to the CH_3 group of saturated carbon and the peak in the range of 1.0–1.3 ppm corresponded to the CH_2 and CH of saturated PIP. When the hydrogenation degree reached 94% as shown in Figure 2(c), the peak at 5.15 ppm belonging to unsaturated carbon shows a very

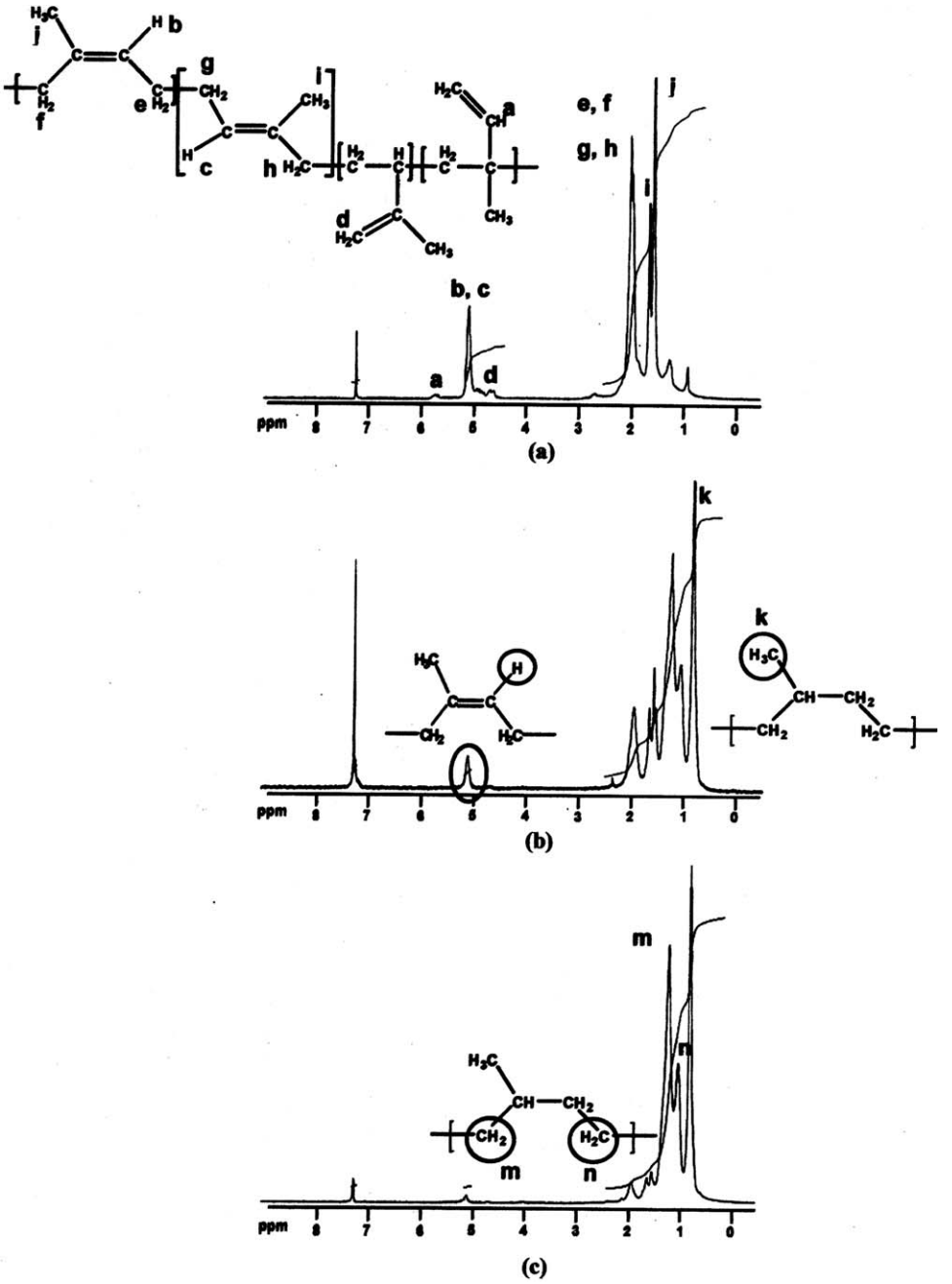

Figure 2. ^{1}H-NMR spectra of (a) PIP, (b) HPIP (78%), and (c) HPIP (94%).

low intensity signal while the peak area of saturated carbon centered at 0.8–1.3 was sharply increased. The peak area of methylene groups for 1,4-polyisoprene appearing from 1.95 to 2.15 ppm dramatically decreased.

According to the NMR spectra, the double bond conversion of the different structure configurations was also evaluated. The results imply that the vinyl-1,2-polyisoprene is firstly saturated followed by 3,4-polyisoprene and 1,4-polyisoprene as a result of the structure hindrance of the methyl group in the 3,4-polyisoprene which tends to impede the reaction between diimide and the double bond in the coordination step of the diimide hydrogenation cycle. Conversely, 1,4 addition of *cis*-polyisoprene and *trans*-polyisoprene were hydrogenated at a slower rate due to the steric effect of PIP chain in the *cis*-, *trans*-structures. This indicated that the diimide species could react with the external double bond of the vinyl groups (1,2- and 3,4-polyisoprene) at the end of polymer chain more effectively than the internal double bond (1,4-polyisoprene), resulting in a high degree of hydrogenation. In addition, it is observed that the reduction of the peak area at 1.58 ppm (*cis*-1,4-polyisoprene) is higher than the intense signal at 1.67 ppm (*trans*-1,4-polyisoprene), indicating that the structure of the *cis* configuration is hydrogenated to a greater extent than that of the *trans*-1,4-polyisoprene. This

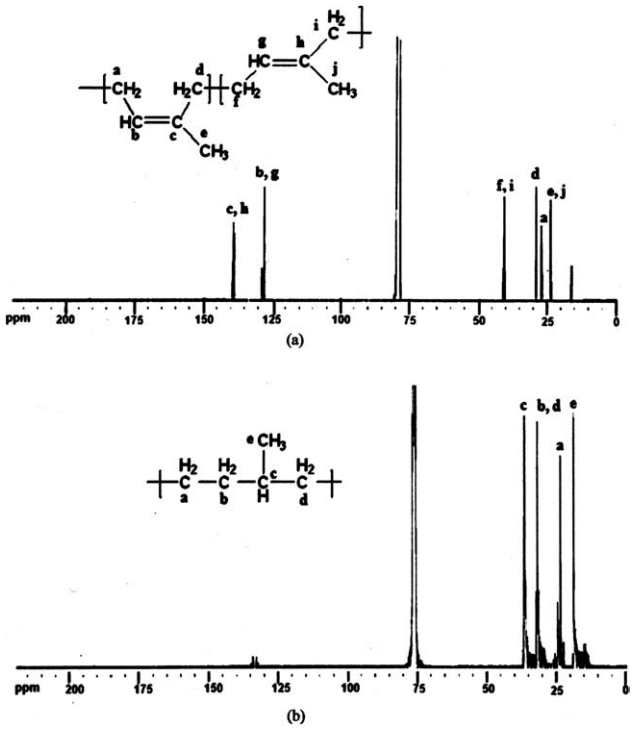

Figure 3. ^{13}C-NMR spectra of (a) PIP and (b) 94% EPM.

selectivity was determined by the ability of saturation of different types of double bonds with diimide. The mechanism of dimide approaching the double bond is believed to occur through a syn-addition, thus, steric hindrance significantly affected the coordination and insertion steps for diimide hydrogenation.

Molecular structure confirmation of the PIP and EPM at 94% conversion was identified by ^{13}C-NMR spectroscopy as shown in Figure 3. For the PIP structure [Figure 3(a)], the peaks at 139.3 ppm were attributed to the unsaturated carbon of *cis*-polyisoprene and *trans*-polyisoprene, and the signal at 125.7 and 125.9 ppm was attributed to the —CH of the unsaturated carbon of the *cis*- and *trans*-polyisoprene, respectively. The chemical shift of 39.8 and 40.0 ppm corresponded to the —CH_2 of *trans*-polyisoprene while the peak at 26.8 and 28.0 ppm belonged to the —CH_2 of *cis*-polyisoprene. The methyl groups of *cis*- and *trans*-polyisoprene are positioned at 23.4 ppm and the —CH_3 of vinyl-polyisoprene are centered at 17.0 ppm. After PIP hydrogenation, the peak in the region of 124–135 ppm corresponding to unsaturated carbon disappeared [Figure 3(b)]. In addition, the new peaks appearing at 19.7, 33.0, and 37.4 ppm were attributed to —CH_3, CH_2, and CH of the propylene unit. The peaks at 33.0 and 24.5 ppm were attributed to CH_2 of the ethylene unit. It is noted that for HPIP at 94% hydrogenation, the structure of an alternating ethylene–propylene copolymer is confirmed by NMR spectroscopy.

Diimide Hydrogenation of Nanosized PIP

The influence of process variables on PIP hydrogenation was studied by varying hydrazine concentration, hydrogen peroxide concentration, amount of boric acid addition, ratio of hydrogen peroxide to hydrazine, water content, and reaction temperature. The effects of all parameters are discussed in detail below.

Effect of Boric Acid Concentration. Boric acid was added into the hydrogenation system to improve the diimide hydrogenation. The effect of boric acid concentration was studied over the range of 0.02–0.15 mol/L. Figure 4 shows that the hydrogenation degree is linearly proportional to the boric acid concentration. This phenomenon illustrated that boric acid could promote hydrogenation with a high selectivity and could reduce the diimide side reactions such as, disproportionation and decomposition as presented in eqs. (2) and (3), respectively.

$$2N_2H_2 \rightarrow N_2H_4 + N_2 \quad (2)$$

$$N_2H_2 \rightarrow N_2 + H_2 \quad (3)$$

Without boric acid addition, the PIP conversion could not reach 60% in 4 h, suggesting that a small amount of boric acid is necessary to accelerate the reaction of hydrogen peroxide dissociation and to induce the diffusion of the diimide active species from the interphase between the water phase and the rubber phase. Lin et al.[27] studied the diimide hydrogenation of NBR latex and reported that the efficiency of hydrogenation using copper ion, silver ion, and ferrous ion as catalysts was lower than that achieved with boric acid addition.

Effect of Hydrazine Monohydrate and Hydrogen Peroxide Concentration. Hydrazine was used as source for releasing the diimide species. The dependence of the percentage of hydrogenation (%HD) on hydrazine concentration was studied over the range of 0.5–6 mol/L. From Figure 5(a), the degree of hydrogenation is seen to increase with an increase in hydrazine concentration from 0.5 to 4 mol/L and a maximum PIP conversion of 78% was achieved. This can be explained in that with increasing hydrazine concentration, a high amount of diimide molecules are generated in the system through a redox reaction

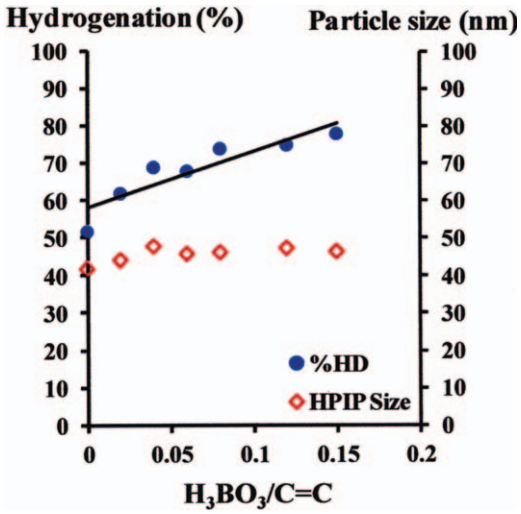

Figure 4. Effect of boric acid addition on PIP hydrogenation. Condition: [N_2H_4], 3 mol/L; [H_2O_2], 4.5 mol/L; [C=C], 1 mol/L; [H_2O], 10 mol/L; *T*, 70°C; time, 4 h. [Color figure can be viewed in the online issue, which is available at wileyonlinelibrary.com.]

Applied Polymer SCIENCE

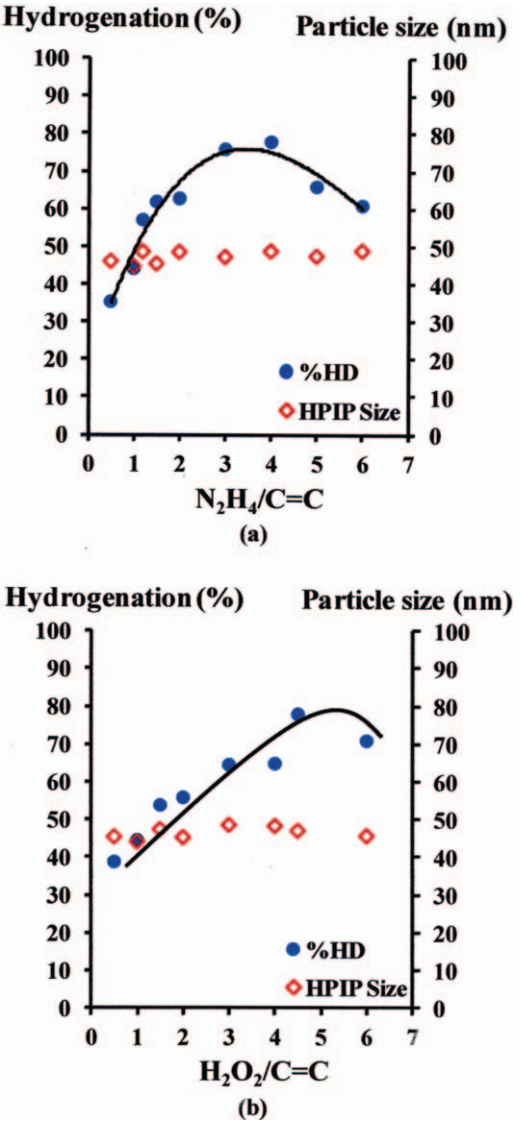

Figure 5. PIP hydrogenation: (a) effect of hydrazine concentration on PIP hydrogenation at $[H_2O_2]$ = 4.5 mol/L. (b) Effect of hydrogen peroxide amount on PIP hydrogenation at $[N_2H_4]$ = 3 mol/L. Condition: $[H_3BO_3]$, 0.15 mol/L; [C[dbondC], 1 mol/L; $[H_2O]$, 10 mol/L; *T*, 70°C; time, 4 h. [Color figure can be viewed in the online issue, which is available at wileyonlinelibrary.com.]

with hydrogen peroxide according to eq. (4). More diimide species would attach to the unsaturated polymer chains resulting in increasing hydrogenation of the carbon double bonds in the nanosized PIP units [eq. (5)]. Conversely, above 4 mol/L of hydrazine, the degree of hydrogenation is suppressed due to the side reaction of the diimide reduction according to eq. (2). Moreover, the particle size slightly increased from 42 nm for PIP to 47 nm for HPIP at 78% hydrogenation.

$$N_2H_4 + H_2O_2 \rightarrow N_2H_2 + 2H_2O \quad (4)$$

$$N_2H_2 + -H_2C - HC = CCH_3CH_2- \rightarrow -H_2C - H_2C - CHCH_3CH_2 - + N_2 \quad (5)$$

For the redox reaction, hydrogen peroxide was used as a strong oxidizing agent to react with the hydrazine molecule. The effect of hydrogen peroxide concentration on PIP conversion has been studied under a hydrazine concentration of 3 mol/L and boric acid of 0.15 mol/L. The phenomenon of increasing hydrogenation level with increasing hydrogen peroxide concentration is shown in Figure 5(b). It was found that the percentage of hydrogenation is sharply increased from 40 to 80% over the studied range of hydrogen peroxide concentration and then decreased, whereas the particle diameter of the hydrogenated product essentially did not change. Hence, hydrogen peroxide should be provided at a sufficient level for oxidizing the hydrazine molecules to release the diimide species. However, the decreasing hydrogenation degree at a high level of hydrogen peroxide (above 4.5 mol/L hydrogen peroxide) was due to the side reaction of hydrogen peroxide as shown in eqs. (6)–(8). Moreover, the high content of hydrogen peroxide in the system possibly tends to cause a crosslinking reaction and forms gel in the rubber latex resulting in a lower hydrogenation efficiency,[28] suggesting that an appropriate hydrogen peroxide concentration is important for double bond reduction and to increase the efficiency of the EPM preparation.

$$2H_2O_2 + N_2H_4 \rightarrow N_2 + 4H_2O \quad (6)$$

$$H_2O_2 + N_2H_2 \rightarrow N_2 + 2H_2O \quad (7)$$

$$2H_2O_2 \rightarrow O_2 + 2H_2O \quad (8)$$

Effect of Hydrogen Peroxide to Hydrazine Ratio. The hydrogen peroxide to hydrazine ratio has a significant effect on the double bond reduction as shown in Figure 6. The hydrogenation degree was increased from 50 to 78% with an increasing ratio of hydrogen peroxide to hydrazine from 0.4 : 1 to 1.5 : 1, whereafter the hydrogenation degree was suppressed. From eq. (4), the ratio of hydrogen peroxide to hydrazine should be 1 : 1 based on stoichiometry. However, the maximum PIP conversion

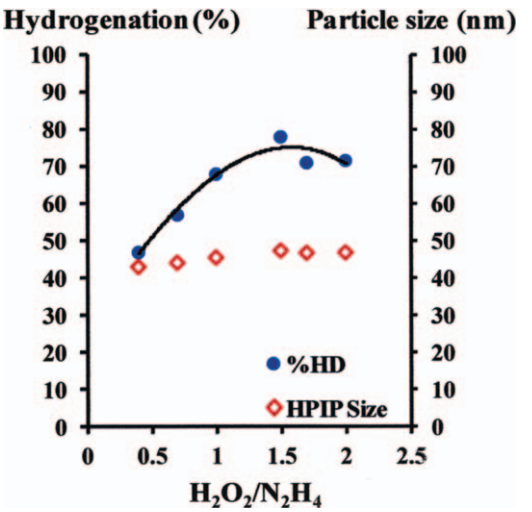

Figure 6. Effect of hydrogen peroxide to hydrazine ratio on PIP hydrogenation. Condition: $[N_2H_4]$, 3 mol/L; $[H_3BO_3]$, 0.15 mol/L; [C=C], 1 mol/L; $[H_2O]$, 10 mol/L; *T*, 70°C; time, 4 h. [Color figure can be viewed in the online issue, which is available at wileyonlinelibrary.com.]

Table I. Effect of Hydrazine Amount on Hydrogenation at the Constant $[H_2O_2]/[N_2H_4]$[a]

N_2H_4 (mol)	H_2O_2 (mol)	Degree of hydrogenation (%)	Particle diameter (nm)
2	3	65.9	46.8
3	4.5	78.0	47.4
4	6	83.2	48.2
5	7.5	87.0	47.5
6	9	87.4	49.0

[a]Condition: PIP particle size, 42 nm; $[H_2O_2]/[N_2H_4]$, 1.5/1; $[H_3BO_3]$, 0.15 mol/L; [C=C], 1 mol/L; $[H_2O]$, 10 mol/L; *T*, 70°C; time, 4 h.

was achieved at a ratio of hydrogen peroxide to hydrazine of 1.5 : 1. It can be implied that hydrogen peroxide could be decomposed easily by reacting with hydrazine or diimide molecule. Therefore, the ratio of hydrogen peroxide to hydrazine needs to be higher than 1 : 1 to enhance effective diimide production. From previous work, it was found that NBR[17] and SBR[28] were effectively hydrogenated at a ratio of hydrogen peroxide to hydrazine of 2 : 1. In this work, the ratio of hydrogen peroxide to hydrazine was 1.5 : 1 since the diimide active molecule was able to effectively attach with a double bond in an inner portion of nanosized PIP compared with the larger particle size and higher steric hindrance exhibited by NBR and SBR.

On a comparison of the effect of hydrazine concentration [Figure 5(a)] and hydrogen peroxide concentration [Figure 5(b)], it is seen that the ratio of hydrogen peroxide to hydrazine was not held constant resulting in a decrease in hydrogenation degree even though hydrazine hydrate concentration was increased. Hence, it is necessary to study the effect of hydrazine concentration on diimide reduction at a constant ratio of hydrogen peroxide to hydrazine of 1.5 : 1. It was found that the hydrogenation level increased sharply from 66 to 87% with an increase in the hydrazine concentration from 2 to 5 mol/L and then slightly increased (Table I). The high hydrogenation degree (87%) was achieved at a concentration of hydrazine and hydrogen peroxide of 5 and 7.5 mol/L, respectively.

Effect of Reaction Temperature. The effect of reaction temperature was studied over the range of 40–80°C. From Figure 7, the increase in reaction temperature dramatically affected the decrease of the carbon double bonds in the PIP structure. When the reaction temperature was increased from 40 to 80°C, the hydrogenation degree was increased from 40 up to 90%, whereas, the PIP hydrogenation conversion did not reach 70% when the reaction temperature was below 65°C. The high temperature could increase the probability of collision between the starting reactants with the polymer chains and accelerate the diimide mobility to coordinate with the double bonds,[17] resulting in a high EPM yield. However, even though high temperature became necessary to obtain a high level of diimide, the particle size was also changed with increasing temperature. For PIP of 42 nm, the particle size was increased from 42 to 50 nm for the resulting HPIP with increasing temperature due to the entanglement of the polymer chains induced by the hydrogenation reaction at high temperature. Hence, an optimum reaction temperature of 70°C was preferred and a high EPM yield (87%) and a relative small particle size (47 nm) were achieved.

Effect of Water Addition. Deionized water was added into the reaction system to reduce the viscosity of the synthetic PIP latex. Figure 8 shows that on increasing the water content in the system, a linear decrease in the hydrogenation level resulted. The high hydrogenation level of 88% was achieved at a water content of 7 mol/L. Although the presence of water in the system could reduce the viscosity of the latex and increase the attachment between the polymer particles and other substances,

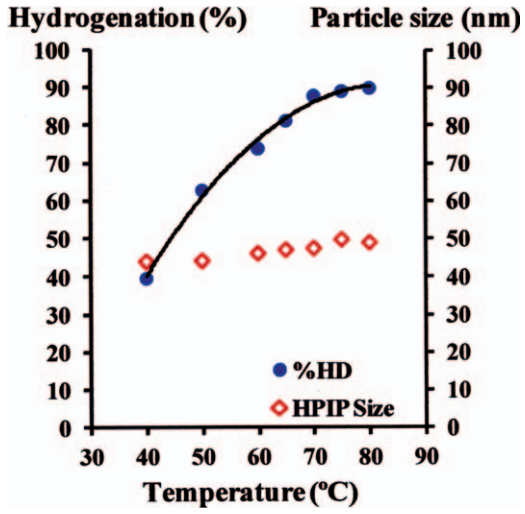

Figure 7. Effect of reaction temperature on PIP hydrogenation. Condition: $[N_2H_4]$, 5 mol/L; $[H_2O_2]$, 7.5 mol/L; $[H_3BO_3]$, 0.15 mol/L; [C=C], 1 mol/L; $[H_2O]$, 10 mol/L; time, 4 h. [Color figure can be viewed in the online issue, which is available at wileyonlinelibrary.com.]

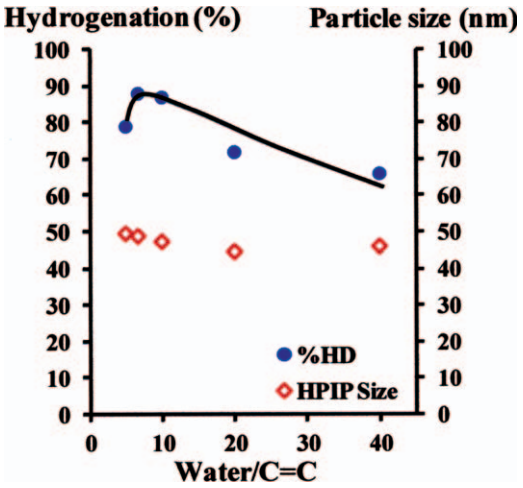

Figure 8. Effect of water addition on PIP hydrogenation. Condition: $[N_2H_4]$, 5 mol/L; $[H_2O_2]$, 7.5 mol/L; [C=C], 1 mol/L; $[H_3BO_3]$, 0.15 mol/L; *T*, 70°C; time, 4 h. [Color figure can be viewed in the online issue, which is available at wileyonlinelibrary.com.]

Applied Polymer SCIENCE

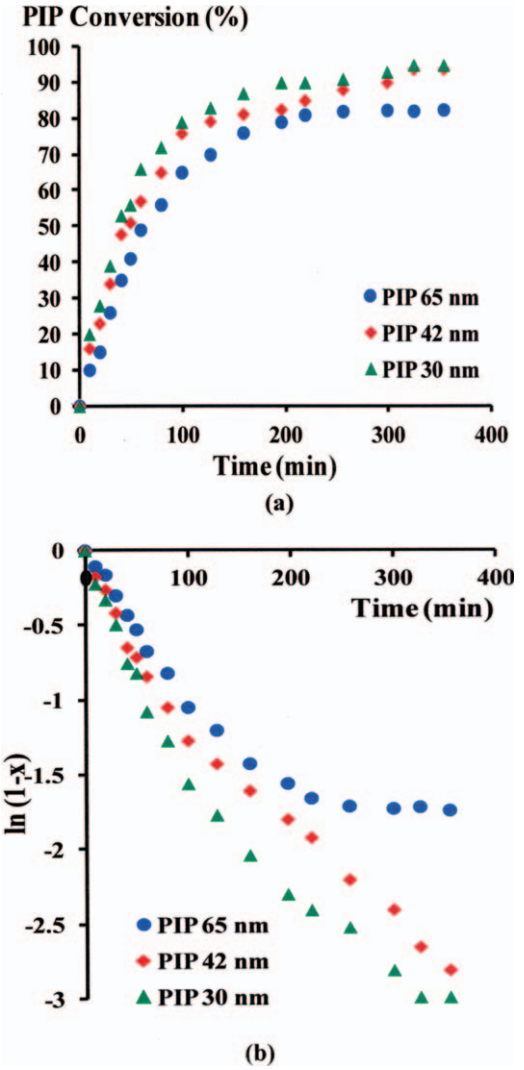

Figure 9. (a) Conversion profile and (b) first order in ln plot of PIP hydrogenation. Condition: [N_2H_4], 5 mol/L; [H_2O_2], 7.5 mol/L; [C=C], 1 mol/L; [H_3BO_3], 0.15 mol/L; [H_2O], 10 mol/L; *T*, 70°C. [Color figure can be viewed in the online issue, which is available at wileyonlinelibrary.com.]

the hydrogenation level was decreased at water content above 20 mol/L. Based on dry rubber content (DRC, the water concentration of 5, 7, 10, 20, and 40 mol/L is equivalent to 13, 9.5, 6.7, 3, and 1.6% DRC, respectively. It can be seen that the hydrogenation degree increased from 66 to 87% with increasing DRC from 1.6 to 6.7% and then decreased to 78% at DRC of 13%. This can be explained that the reaction between hydrazine and hydrogen peroxide occurred in the aqueous phase; thus, the diimide active species was produced in the water phase at high water content (low %DRC) and the diimide migration into the rubber phase was limited, and consequently the hydrogenation efficiency was reduced.[19]

Conversion Profile of Nanosized PIP Hydrogenation

The PIP conversion versus reaction time profile at various particle diameters of PIP was studied over an interval of time from 0 to 5 h [Figure 9(a)]. The double bond conversion was sharply increased with time initially, and then leveled off. It is suggested that diimide is a highly active intermediate species and is consumed toward the surface of the unsaturated rubber particles, so the reduction of the double bonds is observed. For reaction times above 5 h, the PIP conversion remained constant, implying that the mobility of the diimide was retarded in transferring to the carbon double bonds within the particles due to a mass transfer limitation.[29] The dependence on the particle size (30–65 nm) showed that double bond reduction of small particles was higher than that of large size, suggesting that diimide hydrogenation occurred at the outer surface and transferred to the inner particles. Therefore, diimide diffusion was enhanced toward C=C inside smaller particles at a higher rate than that for larger particles resulting in an increase in double bond conversion. According to the layer model for diimide hydrogenation reported by Lin et al.,[30] the double bond reduction was performed from the outer layer and then into the inner particle, so it is suggested that the particles of synthetic PIP should be less than 50 nm to achieve a high degree of hydrogenation. This is due to the fact that the high surface area of the PIP nanoparticles can be attached with diimide active species effectively and the diimide molecule can diffuse toward the double bonds inside the particle, resulting in an increase in EPM yield.

The kinetics of hydrogenation of nanosized PIP at various particle size was also investigated. From Figure 9(b), the hydrogenation rate exhibits an apparent first-order rate law dependence on the double bond substrate concentration, as described by eq. (9).The experimental rate law for the reaction could be written as

$$\frac{d[\mathrm{C=C}]}{dt} = -k'[\mathrm{N_2H_2}][\mathrm{C=C}] \tag{9}$$

When diimide is a highly active intermediate, a pseudo steady-state assumption is made, therefore, the rate of hydrogenation has a first-order dependence on double bond concentration.

The fractional hydrogenation conversion, x is defined as

$$x = 1 - [\mathrm{C=C}]_t/[\mathrm{C=C}]_0, \tag{10}$$

where $[\mathrm{C=C}]_t$ is the double bond concentration at reaction time t and $[\mathrm{C=C}]_0$ is the initial double bond concentration.

Equations (9) and (10) can further be expressed in term of eq. (11)

$$\ln(1-x) = -k't \tag{11}$$

Plots of $\ln(1 - x)$ versus time fit first-order kinetics very well, and thus, the rate constant (k') is determined from the slope of these kinetic profiles. It was found that the rate constant for hydrogenation of PIP of 30, 42, and 65 nm was 16.0×10^5, 13.0×10^5, and 9.9×10^5 (s^{-1}), respectively. Previous work reported that the rate constant of NRL[19] and skim NRL (SNRL)[20] hydrogenation using diimide reduction was 5.4×10^5 and 5.96×10^5 (s^{-1}), respectively. Hence, the higher rate of diimide hydrogenation for PIP nanoparticles was achieved due to the smaller particle size of PIP compared with NRL.

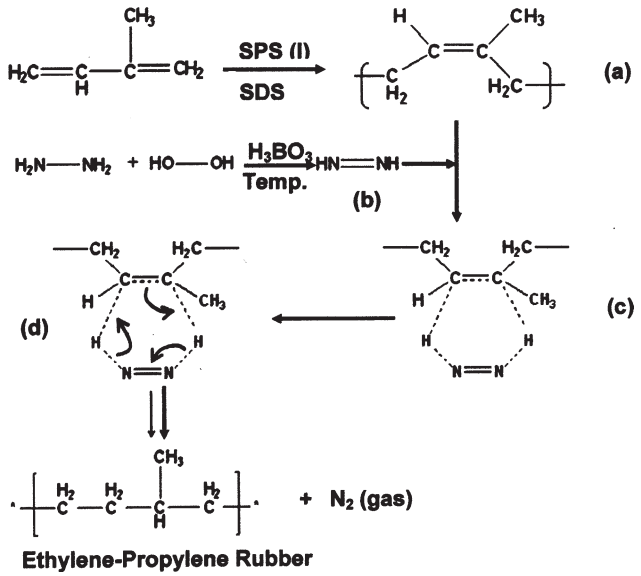

Scheme 1. Proposed synthetic route for nanosized EPM synthesis by diimide hydrogenation of PIP.

Proposed Synthetic Route for Nanosized EPM Synthesis via Diimide Hydrogenation

A synthetic route for the synthesis of nanosized EPM is proposed in Scheme 1. The preparation of nanosized EPM was synthesized through differential microemulsion polymerization to produce synthetic PIP and then diimide hydrogenation was performed to produce EPM. First, IP monomer is polymerized through a radical chain polymerization mechanism to obtain PIP nanoparticles [Scheme 1(a)]. For diimide hydrogenation, hydrogen peroxide as a strong oxidizing agent is used to oxidize hydrazine hydrate via a redox system and subsequently the diimide molecule is released at the interphase [Scheme 1(b)]. This step is accelerated under thermal dissociation of hydrazine which is promoted by boric acid. Then, nanosized particles containing 1,4-PIP (91%) are reacted with the diimide molecule through a coordination process [Scheme 1(c)]. Indeed, the ability of the unsaturated carbon–carbon bonds to coordinate with the diimide species depends on the structure of configuration of the synthetic PIP. Thus, this coordination step would control the configuration of product due to the selectivity between the intermediate diimide molecule and the different double bond structures, suggesting that vinyl PIP is hydrogenated more readily than *cis*-, *trans*-PIP due to steric effects as described in the previous section. After the coordination step, hydrogen is transferred through a hydride shift mechanism toward the olefinic bond to obtain an alkyl complex, and then, the alkyl bond is cleaved by a transferred hydride in an insertion step and nitrogen gas is released [Scheme 1(d)]. Alternatively, the hydrogen atoms for the diimide may transfer to the carbons of double bonds via a four center intermediate with release of nitrogen. Finally, the nanosized EPM latex is successfully obtained via diimide hydrogenation of PIP nanoparticles.

Thermal Analysis of EPM

Thermal properties of the HPIP product at various hydrogenation levels were investigated using TG analysis. From Figure 10,

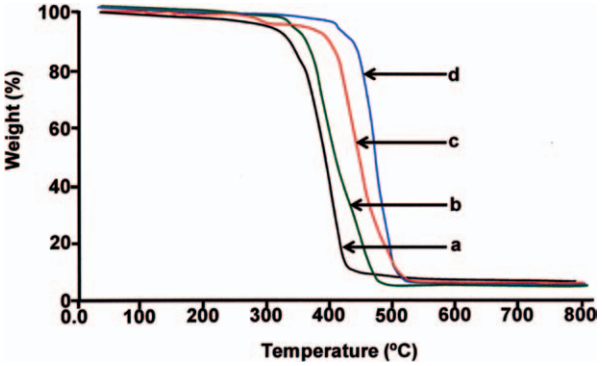

Figure 10. Thermogram of (a) nanosized PIP, (b) HPIP (57%), (c) HPIP (78%), and (d) HPIP (94%). [Color figure can be viewed in the online issue, which is available at wileyonlinelibrary.com.]

the thermograms of PIP and HPIP show a one-step polymer degradation and provide smooth weight loss curves. The T_{id} and the maximum decomposition temperature (T_{max}) are summarized in Table II. PIP of 30 nm had a T_{max} of 425°C while both T_{id} and T_{max} of all HPIP products are higher than that of PIP. It is noted that the degradation temperature increased with an increasing hydrogenation level. When the extent of hydrogenation increased from 57 to 94%, the T_{max} increased from 450 to 510°C. This implied that thermal stability of nanosized PIP depended on the density of the carbon–carbon double bonds. The sigma bonds are stronger than π bonds because the sigma bonds contain hybridized atomic orbitals. Therefore, hydrogenation involves the breaking of π bonds with a change to sigma bonds resulting in an increase in thermal stability of the HPIP nanoparticles. On comparison with commercial ethylene–propylene with an ethlyene/propylene ratio of 1 : 1, the decomposition temperature of nanosized EPM (510°C) was somewhat higher than that of commercial EPM (471°C). Therefore, diimide hydrogenation of nanosized PIP rubber leads to a structure of an alternating ethylene–propylene copolymer having improved thermal stability.

Dynamic Mechanical Properties of HPIP

The elastic modulus of a rubber and its mechanical damping or energy dissipation characteristics as a function of frequency and temperature can be measured by dynamic mechanical analysis. The storage modulus or elastic modulus is measured from the

Table II. Glass Transition Temperature and Decomposition Temperature of Rubber Samples

Rubber	Hydrogenation (%)	T_g (°C)	T_{id} (°C)	T_{max} (°C)
PIP	-	−59.9	359.7	425.4
HPIP	57	−47.9	373.5	450.1
	78	−46.1	422.6	480.9
	94	−42.4	447.3	510.1
EPDM[a]	-	−44.6	452.7	470.7

[a]EPDM has an ethylene:propylene ratio of 50 : 50 and diene content of 9.5%.

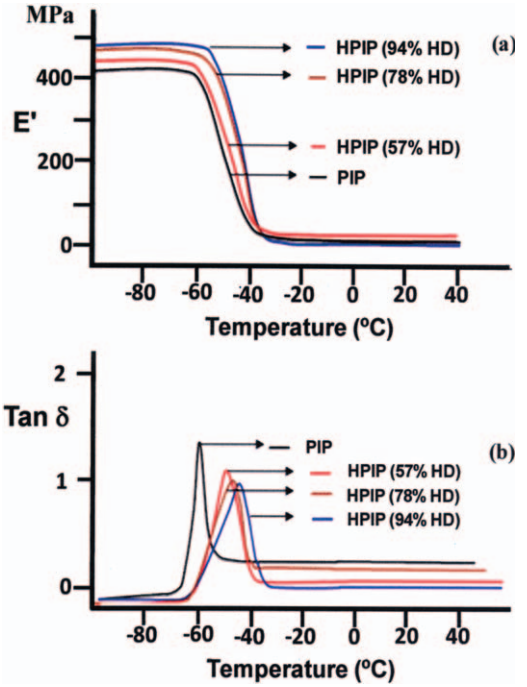

Figure 11. Temperature dependence of (a) storage modulus (E') and (b) loss tangent (tan δ) for PIP and HPIP. [Color figure can be viewed in the online issue, which is available at wileyonlinelibrary.com.]

elastic energy storage of the rubber, indicating the stiffness of materials. From Figure 11(a), it is seen that the storage modulus of PIP and HPIP was decreased with an increase in temperature and rapidly decreased in the transition region due to the mobility and deformation of the polymer chains under the action of an external force. HPIP at 57, 78, and 94% hydrogenation had a storage modulus of 451, 486, and 493 MPa, respectively, and the storage modulus of all HPIP samples was higher than that of PIP (430 MPa). The improvement of storage modulus properties is due to the domains of poly(ethylene-*co*-propylene) segments produced from hydrogenation of the IP unit. Moreover, when PIP was hydrogenated, the free volume and mobility are decreased by the replacement of the ethylene and propylene units resulting in a stronger effective interaction of the molecular chains and high stiffness of the EPM.

The tan $\delta$is determined from the ratio of dynamic loss modulus (E'') to storage modulus (E'). From Figure 11(b), HPIP at 94% hydrogenation showed a lower tan δ than pure PIP which indicated that HPIP had low dynamic loss or low viscous modulus due to a high interaction of the ethylene–propylene segments in the polymer chain.

The T_g could be determined from the center of the peak of the tan δ curves and is summarized in Table II. PIP and HPIP had a single T_g. The T_g value of HPIP increased over the range of 13–20°C compared with PIP. On hydrogenation, T_g of HPIP gradually increased from -59.9 to -42.4°C with an increase in hydrogenation level from 0 to 94%. This result was due to the gradual replacement of amorphous segments of PIP by crystalline ethylene segments in the structure of HPIP. A similar shift in T_g from -31 to -11°C was observed for XSBR at 0 and 80% hydrogenation, respectively.[24] In comparison with EPDM rubber, the T_g of 94% EPM nanoparticle is close to EPDM rubber ($T_g = 44.6$°C).

CONCLUSIONS

EPM nanoparticles with a particle size of 47 nm were successfully synthesized from nanosized PIP via diimide hydrogenation in the presence of hydrazine and hydrogen peroxide using boric acid as promotor. The concentration of boric acid exhibited a beneficial effect on the EPM yield whereas, water addition showed an inverse behavior on the hydrogenation level. The highest hydrogenation degree of 94% was achieved at hydrogen peroxide to hydrazine ratio of 1.5 : 1, boric acid concentration of 0.15 mol/L, and reaction temperature of 70°C. Because of the nanosized PIP, the hydrogenation became more effective for EPM synthesis. This was also confirmed from the hydrogenation rate constant of 30 nm PIP in that it was 1.62 times that of a 65 nm PIP as a result of a mass transfer limitation effect. The 94% EPM product had high thermal stability and provided the T_{max} of 510°C. In addition, the EPM product had the highest storage modulus (493 MPa) due to the replacement of the ethylene and propylene units. Therefore, the proposed alternative route could prepare EPM nanoparticles in the absence of solvent and metal catalyst and is of importance for production of potential rubber product.

Support from the Thailand Research Fund (through the Royal Golden Jubilee Project), Graduate School, Chulalongkorn University, the Natural Sciences and Engineering Research Council of Canada (NSERC), the Thai Government Stimulus Package 2 (TKK2555) under the Project for Establishment of Comprehensive Center for Innovative Food, Health Products and Agriculture and the National Research University Project of CHE and Ratchadaphiseksomphot Endowment Fund (AM1024I) are gratefully acknowledged. The authors wish to express their appreciation to Dr. Bunthita Suppaibulsuk for her assistance and suggestions.

REFERENCES

1. Gamlin, C.; Markovic, M. G.; Dutta, N. K.; Choudhurry, N. R.; Matisons, J. G. *J. Therm. Anal. Cal.* **2000,** *59*, 319.
2. Vostovich, J. E. U.S. Pat.4,303,574, **1981.**
3. Mitra, S.; Ghanbari-Siahkali, A.; Kingshott, P.; Hvilsted, S.; Almdal, K. *Mater. Chem. Phy.* **2006,** *98*, 248.
4. Zhao, Q.; Li, X.; Hu, J.; Ye, Z. *J. Fail. Anal. Prev.* **2010,** *10*, 240.
5. Abdel-Aziz, M. M.; Basfar, A. A. *Polym. Test.* **2000,** *19*, 591.
6. Delor-Jestin, F.; Lacoste, J.; Barrois-Oudin, N.; Cardinet, C.; Lemaire, J. *Polym. Degrad. Stab.* **2000,** *67*, 469.
7. Chen, J.; Wang, G.; Zeng, X.; Zhao, H.; Cao, D.; Yun, J.; Tan, C. K. *J. Appl. Polym. Sci.* **2004,** *94*, 796.
8. Seurer, B.; Bryan Coughlin, E. *Macromol. Chem. Phys.* **2008,** *209*, 1198.
9. Caines, T. L.; Junker, M. L. U.S. Pat.5,384,371,**1995.**
10. Schrage, A.; Schoenberg, J. E. U.S. Pat.3,671,505, **1972.**

11. Eisinger, R. S.; Lee, K. H.; Hussein, F. D.; Zilker, D. P. U.S. Pat.6,011,128, **2000.**
12. Ver Strate, G.; Cozewith, C.; Ju, S. *Macromolecules* **1988,** *21*, 3360.
13. Coutinho, F. M. B.; Xavier, J. L. L. *Polym. Bull.* **1997,** *39*, 133.
14. De Rosa, C.; Auriemma, F.; Ballesteros, O. R.; Resconi, L.; Camurati, I. *Chem. Mater.* **2007,** *19*, 5122.
15. Caballero, M. J.; Suarez, I.; Coto, B.; Grieken, R. V.; Monrabal, B. *Macromol. Symp.* **2007,** *257*, 122.
16. Wideman, L. G. U.S. Pat.4,452,950, **1984.**
17. Zhou, S.; Bai, H.; Wang, J. *J. Appl. Polym. Sci.* **2004,** *91*, 2072.
18. De Sarkar, M.; De, P. P.; Bhowmick, A. K. *Polymer* **2000,** *41*, 907.
19. Mahittikul, A.; Prasassarakich, P.; Rempel, G. L. *J. Appl. Polym. Sci.* **2007,** *105*, 1188.
20. Simma, K.; Rempel, G. L.; Prasassarakich, P. *Polym. Degrad. Stab.* **2009,** *94*, 1914.
21. Xie, X. L.; Yiu Li, R. K.; Liu, Q. X.; Mai, Y. W. *Polymer* **2004,** *45*, 2793.
22. Kim, S.; Wilkie, C. A. *Polym. Adv. Technol.* **2008,** *19*, 496.
23. Hussain, F.; Hojjati, M.; Okamoto, M.; Gorga, R. E. *J. Compos. Mater.* **2006,** *40*, 1511.
24. Suppaibulsuk, B.; Prasassarakich, P.; Rempel, G. L. *Polym. Adv. Technol.* **2010,** *21*, 467.
25. He, G.; Pan, Q.; Rempel, G. L. *Macromol. Rapid Commun.* **2003,** *24*, 585.
26. Wei, R.; Luo, Y.; Li, Z. *Polymer* **2010,** *51*, 3879.
27. Lin, X.; Pan, Q.; Rempel, G. L. *Appl. Catal. A* **2004,** *276*, 123.
28. Lin, X.; Pan, Q.; Rempel, G. L. *J. Appl. Polym. Sci.* **2005,** *96*, 1122.
29. De Sarkar, M.; De, P. P.; Bhowmick, A. K. *J. Appl. Polym. Sci.* **1997,** *66*, 1151.
30. Lin, X.; Pan, Q.; Rempel, G. L. *Ind. Eng. Chem. Res.* **2006,** *45*, 1300.